energies

MDPI

Article

The Effect of Adjusting Sinter Raw Mix on Dioxins from Iron Ore Co-Sintering with Municipal Solid Waste Incineration Fly Ash

Hao He, Xuanhao Guo, Lizheng Jin, Yaqi Peng *, Minghui Tang and Shengyong Lu

State Key Laboratory for Clean Energy Utilization, Institute for Thermal Power Engineering, Zhejiang University, Hangzhou 310027, China; 21960230@zju.edu.cn (H.H.); 21960572@zju.edu.cn (X.G.); jinlizheng@zju.edu.cn (L.J.); lytmh1214@zju.edu.cn (M.T.); lushy@zju.edu.cn (S.L.)

* Correspondence: pengyaqi@zju.edu.cn; Tel.: +86-18768117994

Abstract: The inhibition effect of calcined lime (CaO) and limestone ($CaCO_3$) on the formation of dioxins during iron ore co-sintering with fly ash was investigated in a sinter pot in the present work. Experimental results indicated that international total toxicity equivalent concentration of dioxins decreased from 1.4335 to 0.2922, 0.1048, 0.4562, and 0.3098 ng I-TEQ Nm^{-3} under four different experimental conditions. It can be concluded that 5 wt.% calcined lime with 3 wt.% limestone is the optimal addition to reduce the concentration of dioxins in flue gas, with 92.70% inhibition efficiency. Effects on dioxin distribution was also analyzed. The distribution proportion of low-chlorinated dioxins was found to increase, while that of high-chlorinated dioxins decreased, except for octachlorianted dibenzo-p-dioxins (OCDD). The reason is that the consumption of HCl not only inhibits the de novo synthesis, but also dramatically promotes the condensation and dechlorination to produce more tetrachlorianted dibenzo-p-dioxins and octachlorianted dibenzo-p-dioxins through precursors. Finally, condensation, dichlorination, and inhibition mechanisms of dioxins during co-sintering with municipal solid waste incineration (MSWI) fly ash are proposed.

Keywords: municipal solid waste incineration fly ash (MSWI FA); PCDD/Fs; iron ore sintering; inhibition

Citation: He, H.; Guo, X.; Jin, L.; Peng, Y.; Tang, M.; Lu, S. The Effect of Adjusting Sinter Raw Mix on Dioxins from Iron Ore Co-Sintering with Municipal Solid Waste Incineration Fly Ash. *Energies* **2022**, *15*, 1136. https://doi.org/10.3390/en15031136

Academic Editor: Giorgio Vilardi

Received: 9 November 2021
Accepted: 28 January 2022
Published: 3 February 2022

1. Introduction

Municipal solid waste incineration (MSWI) [1] has developed rapidly in recent years, and controversy on MSWI's safety to human health and the ecological environment is increasingly fierce, and the public has aroused great concern around the world, especially regarding MSWI fly ash (FA) [2]. MSWI FA is identified as a hazardous waste in many countries as it contains leachable heavy metals and polychlorinated dibenzo-p-dioxins and dibenzofurans (PCDD/Fs) [3]. Many methods have been developed to dispose of fly ash such as landfill, solidification/stabilization, sintering, melting, vitrification, biological/chemical extraction, mechanochemistry, etc. Landfill after cement solidification/stabilization with a chelating agent is the most widespread disposal method, which barely decomposes dioxins, but increases the volume of the waste, causing the consumption of land resources [4,5].

Thermal treatment such as sintering [6,7], melting [8], and vitrification are being developed to dispose MSWI fly ash [9,10] by decomposing dioxins and synergistically solidifying heavy metals. Moreover, this thermal disposal method conforms with the principle of "reducing quantity", "harmless", and that products are environmentally friendly materials that can be reutilized. However, compared with non-thermal treatments, the energy consumption and economic costs are higher, which limits the development of high temperature thermal treatment technology [5,11]. Thus, researchers have shifted more attention to co-disposing processes.

Co-disposal is a solid waste disposal method that replaces one of the raw materials by adding satisfied or pretreated waste to the process in conventional high temperature

production. Co-disposing of MSWI fly ash with the sintering process has been researched over the past decade. The iron ore sintering process is one of the most important procedures of iron and steel production. It provides high quality iron ore raw materials for ironmaking to avoid clogging of the blast-furnace [12,13]. During sintering, materials will go through four stages with the sintering bed, proceeding from the top to the bottom. Previous studies have revealed that dioxins decomposed during combustion due to the high temperatures (>1000 °C) supplied by the combustion of fuels [14], and reformed in the preheat-dry zone, exhibiting a remarkable de novo synthesis pathway [15,16] A great deal of coke, chlorine, and catalytic metals contribute to the de novo synthesis [17,18] since the temperatures range between 200–650 °C [19,20], and fly ash is abundant in these necessary elements in the form of carbon and chlorides [21,22]. Previous research has revealed that the addition of MSWI FA would increase the concentration of dioxins in the flue gas from the sintering process, whether the fly ash is water washed or not [14,23]. Currently, 0.5 ng I-TEQ/Nm^3 (I-TEQ: International Toxic Equivalent Quantity) is the accepted limit in China regulated for the control of PCDD/F emissions from iron ore sinter plants. In order to comply with the increasingly strict emission standards, measures need to be adopted to diminish dioxins from the sintering process including source control, optimum operating conditions, sintering exhaust gas recirculation, additive inhibitors, etc. [24].

The main mechanisms of inhibitors are reacting with chlorine or reducing the catalytic activity of metal catalysts. Nitrogen-based, sulfur-based, and alkali-based are three common inhibitors in some current studies. The sulfur-based inhibitors will increase sulfur oxides such as SO_2 emission in flue gas, and consequently increase the desulfuration burden for the iron and steel industry [25,26]. The mechanism and effect of nitrogen-containing inhibitors, especially urea, added into the iron ore sintering raw mix has already been investigated and verified by many researchers [27,28]. It is reported that alkaline inhibitors such as CaO, $CaCO_3$ can remove HCl and Cl_2 in flue gas to inhibit the PCDD/F formation and emissions [29]. However, the PCDD distribution proportion may remain invariable, increasing or decreasing [30]. Though alkali-based inhibitors are strictly restricted to use during the pig iron production process due to the negative effect on the quality of sinter [24], adjusting its sinter raw mix within the normal range seems feasible [12]. A few studies have focused on the inhibiting behavior of adjusting the sinter raw mix (calcined lime (CaO) and limestone ($CaCO_3$)), but the inhibition mechanisms of CaO or $CaCO_3$ during iron ore co-sintering with MSWI fly ash are still unclear.

Thus, the aim of this study was to find whether adjusting the sinter raw mixture (calcined lime (CaO) and limestone ($CaCO_3$)) is effective at inhibiting the dioxin concentration in flue gas, and focused on the inhibiting behavior of PCDD/Fs to explore the inhibition mechanism. The proportion of calcined lime or limestone in the sinter raw mix was slightly increased (1 wt.%, 2 wt.%) within the normal range to inhibit the reformation of dioxins in the present work. The total PCDD/F emissions and the inhibitory behavior of CaO or $CaCO_3$ on PCDD/F congeners were explored. Finally, probable condensation, dichlorination, and the inhibition mechanisms of dioxins during co-sintering with MSWI fly ash are proposed.

2. Materials and Methods

2.1. MSWI Fly Ash and Sintering Raw Mix

Municipal solid waste incineration fly ash used in this study was sampled from a MSWI grate furnace plant located in Shanghai, China. Washed FA (WFA) was obtained through a three-stage countercurrent washing method with the solid to deionized water ratio of 1/6 [31]. The main elementary components in fly ash was analyzed with X-ray fluorescence (XRF, Thermo-scientific ARL ADVANT'X IntelliPowerTM 4200, Wilmington, DE, USA) and the results are provided in Table 1. The calcium content of the WFA was 44.28%, NaCl and KCl concentrations were significantly reduced after water washing, and the content of chlorine was lower than 2 wt.%, according to the latest industrial standard in China (HJ 1134-2020).

Table 1. Main elementary components of FA and WFA used in the sintering experiments (mass, %). Reprinted with permission from Elsevier, 2022 [32].

Components	Ca	Cl	Na	K	Si	F	Zn	Fe	Cu
FA	47.12	26.45	14.97	3.44	1.77	1.25	0.74	0.38	0.06
WFA	44.28	2.10	0.87	0.41	3.29	2.26	1.42	1.12	0.14

Figure 1 shows the concentration distribution of 17 toxic PCDD/Fs in FA and WFA. The total I-TEQ concentrations of PCDD/Fs in FA and WFA were 302.2 and 599.2 pg I-TEQ/g, respectively, which is consistent with the TEQ concentration of fly ash in other cities in China. OCDD and 1234678-HpCDF were the two dominant congeners, while 23478-PeCDF contributed the highest I-TEQ concentration with 24.2% and 25.5%, respectively.

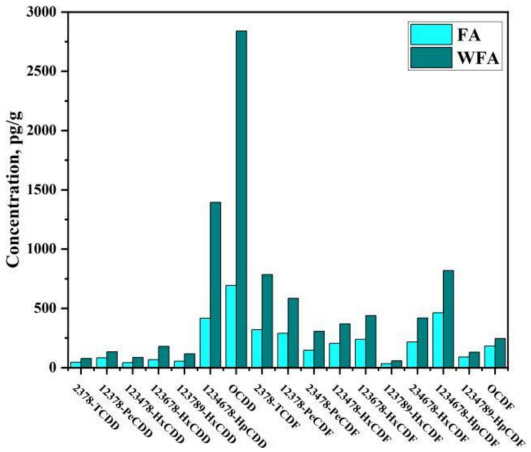

Figure 1. Concentration distribution of 17 toxic PCDD/Fs in FA and WFA.

The raw materials were provided by a sintering plant in Shanghai, China, and the main chemical compositions that were detected according to the Chinese National Standard (GB/T 6730) and the calculated material ratios of the sinter raw mix for different tests are shown in Tables 2 and 3. The experimental condition of flue gas one (FG1) is in accordance with the proportion of the sintering plant where raw materials were sampled, and FG1 is the contrast group to observe the effects of adding fly ash and changing the proportion of raw materials. FG2 is with the addition of 1 wt.% WFA compared to FG1. FG3 and FG4 are conditions increasing the calcined lime (the main component is CaO) in the raw mix by 1 and 2%, respectively, and FG5 and FG6 are conditions increasing the limestone (the main component is $CaCO_3$) by 1 and 2%, respectively. The binary basicity ($w(CaO)/w(SiO_2)$) and coke fine content were 1.9 and 3.5 wt.%, respectively. The ferrous materials were the iron ore fines, mixed iron ore, and recycling materials (return sinter fines). The influence of fly ash, limestone, calcined lime, and dolomite additions were investigated.

Table 2. Chemical compositions of raw materials (mass, wt.%). Reprinted with permission from Elsevier, 2022 [32].

Raw Materials	TFe[a]	FeO	SiO_2	CaO	MgO	Al_2O_3	S	P	Cl	LOI[b]
Mixed iron ore	60.69	3.18	4.37	0.64	0.21	2.27	0.036	0.05	0.11	4.93
Iron ore fines	56.23	6.18	5.93	9.75	1.47	1.2	0.014	0.057	0.039	0.12
Return sinter fines	56.1	5.51	5.81	9.18	1.39	1.93	0.039	0.059	0.049	0.61
Calcined lime	0.25	0.3	6.47	80.63	0.46	0.45	0.14	0.02	0.056	8.79
Limestone	0.39	0.072	0.96	53.75	0.61	0.24	0.012	0.004	0.044	42.11
Dolomite	0.29	0.056	2.2	30.16	20.4	0.01	0.006	0.01	0.050	44.23
Coke breeze	0.00	0.00	10.00	0.00	0.30	0.00	1.03	0.17	0.025	74.00

TFe[a]: Total Fe content; LOI[b]: Loss on ignition at 950 °C in air.

Table 3. The mass ratio of all raw materials (mass, %).

Raw Materials	FG1	FG2	FG3	FG4	FG5	FG6
Mixed iron ore	46.0	46.0	46.0	46.0	46.0	46.0
Iron ore fines	22.1	22.1	22.1	22.1	22.1	22.1
Return sinter fines	18.9	18.9	18.9	18.9	18.9	18.9
Coke breeze	3.5	3.5	3.5	3.5	3.5	3.5
Calcined lime	3.0	3.0	4.0	5.0	3.0	3.0
Limestone	3.0	3.0	3.0	3.0	4.0	5.0
Dolomite	3.5	3.5	2.5	1.5	2.5	1.5
WFA[a]	0	1	1	1	1	1

WFA[a]: Water washed fly ash.

2.2. Experimental Procedures

The experiment was carried out in a sintering pot to simulate the commercial sintering process [23,33]. The sintering process includes proportioning, mixing, granulating, feeding, ignition, and sintering, as illustrated in Figure 2. One wt.% WFA was mixed with the sinter raw mix during the mixing process. Then, the mixture was fed into a drum (Φ 600 mm × 300 mm) for granulating [34]. Following this, a compact bed was created by the granules charged on a 1-kg hearth layer, which was at the bottom of the sinter pot. After this, a mixture of natural-gas and compressed air was used to ignite the sinter raw mixture for 120 s. The sintering process started at approximately 1200 °C and ended when the maximum temperature began to decrease. XAD-II polymeric resin was used to adsorb the dioxins in the tail gas, which was filtrated by a filter membrane, and the rest of the dioxins were collected by two bottles of toluene. Furthermore, toluene was used to wash the sampling pipe twice at the end of each experiment. Finally, the above three materials were combined together for further analysis of dioxins in tail gas. Each test was conducted twice sequentially to ensure the accuracy and reliability of the data [32].

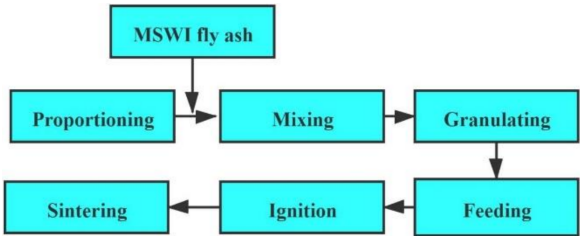

Figure 2. Flow diagram of co-disposing MSWI fly ash through iron ore sintering. Developed from [35].

2.3. Analytical Methods

The procedures of the dioxin analysis in flue gas followed the U.S. EPA methods 1613 and 23A, respectively. After nitrogen-blown, the purified and concentrated extracts were dissolved in 25 uL nonane (spiking with 1 ng of ^{13}C-labelled recovery standards) for the preparation of dioxin analysis. High-resolution gas chromatography/high-resolution mass spectrometry (JMS-800D, JEOL Co., Tokyo, Japan) was used to identify and quantify the concentration of 17 dioxins. Detailed steps of the clean-up procedure can be found in our group's previous studies [36,37].

The international total toxicity equivalent concentration of dioxins is the arithmetic mean value of two parallel samples collected from each experimental condition and the inhibition efficiency can be calculated through Equation (1):

$$I_{effx} = \frac{C_{FG2} - C_{FGx}}{C_{FG2}} \times 100\% \quad (1)$$

where C_{FG2} is the content or the international total toxicity equivalent concentration of dioxins in FG2, ng/Nm^3, or ng I-TEQ/Nm^3; C_{FGx} is the content or the international total toxicity equivalent concentration of dioxins in FG3,4,5,6, respectively, ng/Nm^3 or ng I-TEQ/Nm^3.

Average degree of chlorination (dc) of PCDD/Fs is calculated as:

$$d_c = \sum_{i=4}^{8} f_i \times n_i \quad (2)$$

where f_i is the mass distribution of PCDD-, PCDF-, or PCDD/F-congeners, and n_i is the number of chlorine atoms in PCDD/F molecules.

3. Results and Discussion

3.1. Emissions Reduction in PCDD/Fs

Table 4 shows the I-TEQ value of 17 PCDD/F congeners and the inhibition efficiency for all samples. The I-TEQ value of FG1 (0 wt.% WFA without adjusting its sinter raw mix) was 0.687 ng I-TEQ/Nm^3. After 1 wt.% WFA was added to the sinter raw mix (FG2), the I-TEQ concentration of dioxins in flue gas increased to 1.4335 ng I-TEQ/Nm^3, which was twice as much as that of FG1, showing a significant facilitation in the formation of PCDD/Fs. After adjusting its raw mix ratio in FG2, the I-TEQ concentrations of FG3, FG4, FG5, and FG6 decreased to 0.2922, 0.1048, 0.4562, and 0.3097 ng I-TEQ/Nm^3, respectively. These concentrations were lower than the Chinese limit of 0.5 ng I-TEQ/Nm^3. The inhibition efficiencies were 78.04%, 92.70%, 68.22%, and 78.43%. For all samples, 2,3,4,7,8-PeCDF contributed the greatest toxicity concentration, though the component of it was lower than 1,2,3,4,6,7,8-HpCDF. The above results suggest that the I-TEQ concentration of dioxins during co-sintering were affected by the sinter raw mix. In this study, FG4 (5 wt.% CaO and 3 wt.% $CaCO_3$) showed the highest inhibition efficiency.

Table 4. The I-TEQ concentrations (ng I-TEQ/Nm3) of PCDD/Fs for six experimental flue gas samples.

Classification	Congeners	FG1	FG2	FG3	FG4	FG5	FG6
PCDDs	2378-TCDD	0.0154	0.0378	0.0096	0.0075	0.0136	0.0123
	12378-PeCDD	0.0315	0.0740	0.0211	0.0087	0.0309	0.0295
	123478-HxCDD	0.0067	0.0151	0.0023	0.0008	0.0041	0.0025
	123678-HxCDD	0.0116	0.0252	0.0039	0.0015	0.0050	0.0034
	123789-HxCDD	0.0077	0.0169	0.0041	0.0012	0.0043	0.0028
	1234678-HpCDD	0.0038	0.0093	0.0016	0.0008	0.0022	0.0013
	OCDD	0.0005	0.0011	0.0003	0.0001	0.0004	0.0003
PCDFs	2378-TCDF	0.0443	0.1110	0.0213	0.0110	0.0507	0.0383
	12378-PeCDF	0.0242	0.0571	0.0080	0.0047	0.0168	0.0149
	23478-PeCDF	0.2657	0.5411	0.1235	0.0352	0.1827	0.1023
	123478-HxCDF	0.0901	0.1767	0.0233	0.0104	0.0505	0.0321
	123678-HxCDF	0.0738	0.1529	0.0235	0.0096	0.0349	0.0294
	123789-HxCDF	0.0136	0.0233	0.0058	0.0017	0.0081	0.0049
	234678-HxCDF	0.0796	0.1517	0.0375	0.0091	0.0416	0.0272
	1234678-HpCDF	0.0157	0.0359	0.0055	0.0021	0.0084	0.0072
	1234789-HpCDF	0.0023	0.0052	0.0008	0.0004	0.0017	0.0010
	OCDF	0.0004	0.0012	0.0002	0.0001	0.0004	0.0003
I-TEQ[a]	-	0.6870	1.4355	0.2922	0.1048	0.4562	0.3098
Inhibition efficiency	-	-	-	79.64%	92.70%	68.22%	78.43%

I-TEQ[a]: Average international toxic equivalent.

The I-TEQ emission concentrations of PCDD/Fs are shown in Figure 3a. In FG1, the I-TEQ concentrations of PCDDs and PCDFs were 0.0772 and 0.6098 ng I-TEQ/Nm^3, and PCDFs contributed 88.76% of the I-TEQ concentration. The PCDF/PCDD ratio was 5.28, as listed in Table 5, showing a significant distribution characteristic of PCDD/Fs from the sintering process. Many studies have confirmed that de novo synthesis mainly generates PCDFs, and PCDD congeners were synthesized through the precursor pathway [38]. With the addition of WFA (FG2), the emission I-TEQ concentrations of PCDDs and PCDFs increased to 0.1793 and 1.2562 ng I-TEQ/Nm^3, respectively, and PCDFs con-

tributed 87.51% of the I-TEQ concentrations. By adjusting the raw sinter mix of FG2, the I-TEQ concentrations were 0.0659, 0.0206, 0.0450, and 0.0521 ng I-TEQ/Nm^3 for PCDDs and 0.3004, 0.0843, 0.3956, and 0.2576 ng I-TEQ/Nm^3 for PCDFs, respectively. The inhibition efficiencies of PCDDs and PCDFs are shown in Figure 3b. As shown in this figure, the inhibition efficiencies of PCDDs were 76.07%, 88.53%, 66.26% and 70.93%, respectively. The inhibition efficiencies of PCDFs were 80.15%,93.29%, 68.50%, and 79.49%, respectively. The inhibition efficiencies of PCDDs (PCDFs) increased from 76.07% to 88.53% (from 80.15% to 93.29%) overall whereby the inhibition efficiencies with 4% CaO and 4% $CaCO_3$ addition corresponded to an increase of 76.07% (80.15%) and 66.26% (68.50%), respectively. For 5% CaO and 5% $CaCO_3$, the increment was 88.53% (93.29%) and 70.93% (79.49%), respectively. Evidently, the inhibition efficiency of PCDFs was higher than that of PCDDs. In addition, all 17 toxic dioxins were inhibited by CaO or $CaCO_3$, resulting in a reduction in PCDD/Fs by more than 65%, but CaO seemed to better inhibit the production of PCDD/F compounds.

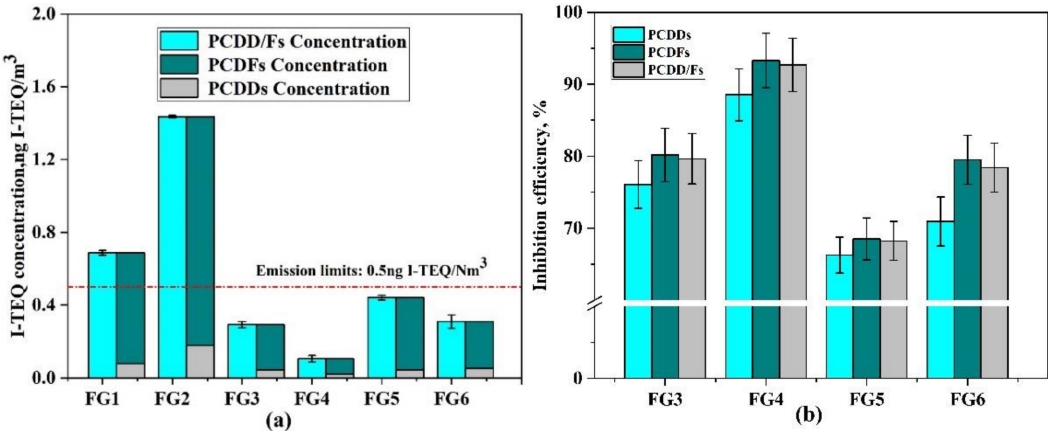

Figure 3. (**a**) I-TEQ concentration of PCDDs and PCDFs; (**b**) inhibition efficiency of PCDDs and PCDFs.

Table 5. Weight average level of chlorination and PCDF/PCDF ratio.

Samples	FG1	FG2	FG3	FG4	FG5	FG6
dc-PCDD	7.03	7.03	7.12	7.07	7.12	7.10
dc-PCDF	6.13	6.15	6.10	6.01	6.02	6.03
dc-PCDD/F	6.27	6.29	6.31	6.24	6.21	6.21
PCDFs/PCDDs	5.28	4.99	3.94	3.63	4.79	4.91

3.2. Effects on PCDD/Fs Congeners

The homologue profiles and the ratio of PCDD/PCDF are affected by adjusting the sinter raw mix. The weight percentage distribution of 17 toxic congeners is shown in Figure 4. OCDD and HpCDD were the dominant congeners in all samples and the percentage of OCDD increased from 38% to 48%, 45%, 48%, and 51% in FG3, FG4, FG5, and FG6, respectively. In this study, the increase in OCDD may be due to the precursor formation of PCDD/Fs catalyzed by Cu or Cr. Similarly, CaO was discovered to facilitate OCDD/TCDD generated from PCP prominently at 850 °C by Lu et al. [30]. In FG3 and FG4, the increase in CaO or CaCO3 reduced the fraction of HpCDD and HxCDD, but slightly increased the mass proportion of low-chlorinated PCDDs, which might be a result of the mutual chlorination of dioxins that was inhibited [26]. Among them, the fraction of HpCDD reduced from 34% to 27%, 31%, 26%, and 23% and HxCDD declined from 21% to 17%, 14%, 16%, and 15%, while PeCDD increased from 5% to 7%, 7%, 7%, and 10% and TCDD increased from 1% to 2%, 3%, 2%, and 2%.

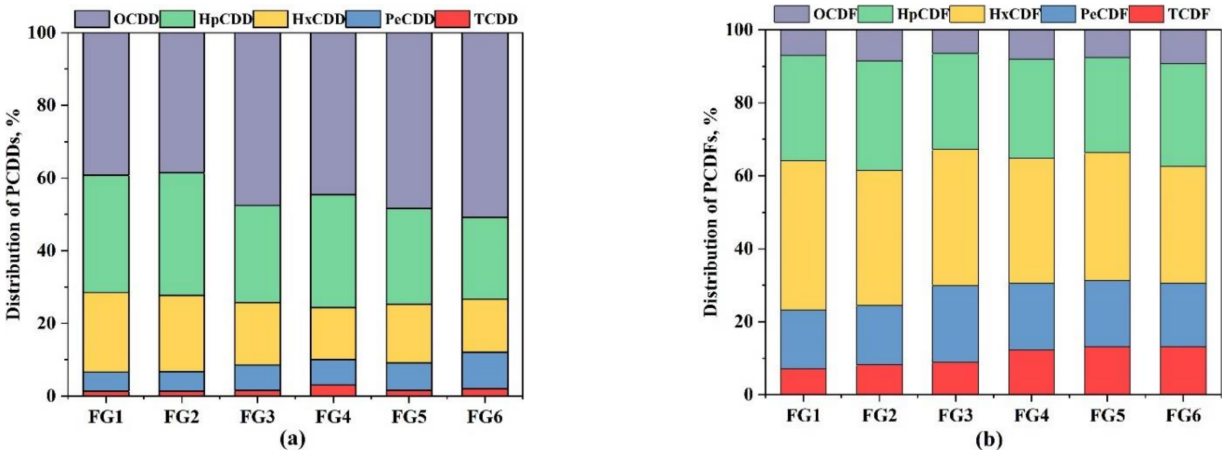

Figure 4. (**a**) Mass distribution of PCDDs; (**b**) mass distribution of PCDFs.

The same phenomena were discovered in the PCDFs except for OCDF, and the increase in CaO or $CaCO_3$ had a slight impact on OCDF. The increase in CaO or $CaCO_3$ decreased the chlorination of PCDFs, especially in FG4 and FG6, due to the inhibition of the de novo formation of dioxins. As shown in Figure 4, the dominant two congeners were HpCDF and HxCDF for all samples. With the addition of CaO and $CaCO_3$, the proportion of HpCDF and HxCDF decreased, while that of PeCDF and TCDF increased.

The inhibition efficiency of CaO/$CaCO_3$ on PCDD and PCDF congeners is compared in Figure 5. There was similar trend between increasing CaO or $CaCO_3$, where the inhibition efficiency of high chlorinated homologues was higher than that of low chlorinated homologues. For example, the inhibition efficiencies of HxCDD (HpCDF) were the highest among PCDDs (PCDFs), resulting in the change in the distribution proportions. Moreover, compared with the FG2 test, the average degree of chlorination of PCDFs decreased after increased CaO or $CaCO_3$, revealing that the de novo formation and chlorination process of PCDFs were inhibited, as shown in Table 5.

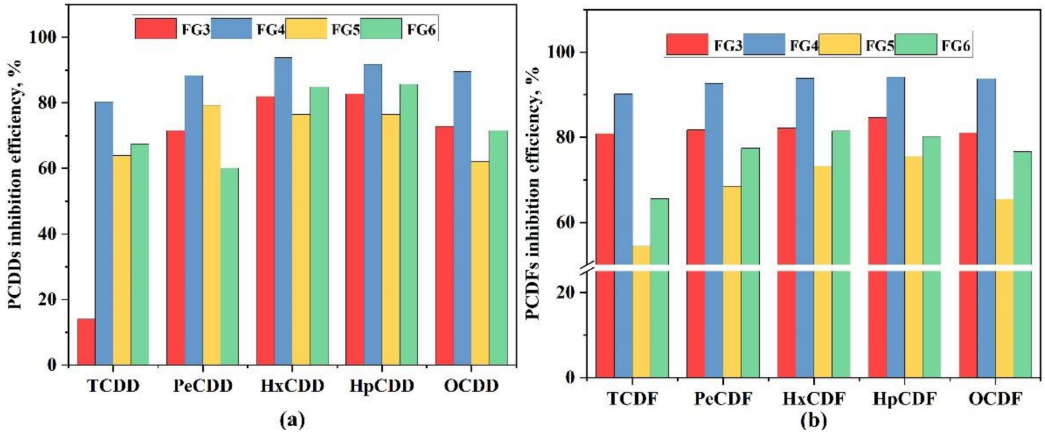

Figure 5. (**a**) The efficiency of PCDD congener inhibition. (**b**) The efficiency of PCDF congener inhibition.

3.3. Inhibition Mechanisms

The formation of PCDD/Fs requires carbon, chlorine, oxygen, and metal catalysts and reducing chlorine and weakening the catalytic activities is beneficial to suppress the formation of PCDD/Fs [39].

For chlorination, the presence of different forms of chlorine had different effects on the synthesis of dioxins [40], since the activation energy of hydrogen in the benzene ring replaced by chlorine with Cl_2 is lower than that with HCl [41,42]. Many studies have confirmed that metal chlorides have a stronger dioxin catalytic capacity than metal oxides,

especially $CuCl_2$, which has the maximum catalytic capacity to boost the conversion of HCl to Cl_2 (Equations (3) and (4)) through the Deacon reaction (Equation (5)).

$$CuO + 2HCl \rightarrow CuCl_2 + 2H_2O \quad (3)$$

$$CuCl_2 + 1/2\ O_2 \rightarrow CuO + Cl_2 \quad (4)$$

$$2HCl + O_2 \rightarrow Cl_2 + H_2O \quad (5)$$

CaO and $CaCO_3$ can react with acidic chlorine (HCl and Cl_2) in the flue gas through Equations (7)–(10). These reactions diminish the concentrations of the chlorine source that is essential to synthesize PCDD/Fs, and inhibit the chlorination of low substituted dioxins. Typically, the decrease in Cl_2 will significantly impede the de novo synthesis. Furthermore, active radicals such as hydrogen radicals (H·) via thermal ionization in the presence of moisture might impede the formation of dioxins or attack the C–l bonds to form aromatic compounds [43,44], as shown in Figure 6. The C–Cl bond is easy to attack by active radicals because too many chlorine atoms would weaken the binding force of C and Cl [45,46].

$$CaO + 2HCl \rightarrow CaCl_2 + H_2O \quad (6)$$

$$2CaO + 2Cl_2 \rightarrow CaCl_2 + Ca(ClO)_2 \quad (7)$$

$$CaCO_3 + 2\ HCl \rightarrow CaCl_2 + H_2O + CO_2 \quad (8)$$

$$2CaCO_3 + 2Cl_2 + 2H_2O \rightarrow CaCl_2 + Ca(HCO_3)_2 + 2\ HClO \quad (9)$$

$$CaO + H_2O + CuCl_2 \rightarrow Cu(OH)_2 + CaCl_2 \quad (10)$$

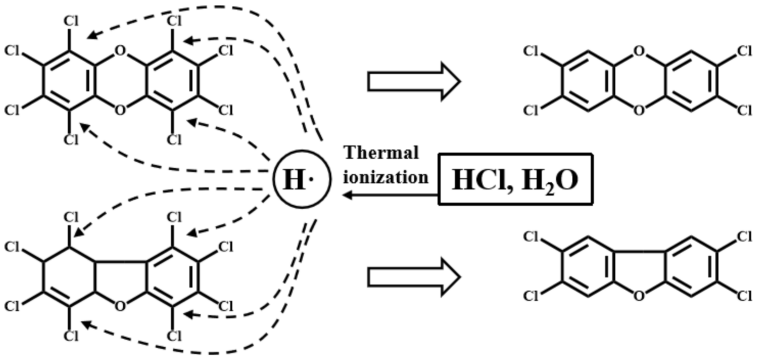

Figure 6. Schematic diagram of the hydrogen radical (H) attacked C–Cl bond on PCDD/Fs molecular.

The results also prove that the chlorine atoms on the longitudinal (1,4,6,9) positions are preferentially removed compared to the chlorine atoms on lateral (2,3,7,8) positions [47]. Specifically, high-chlorinated PCDD/Fs have more Cl atoms on longitudinal positions, making them easy to remove by active radicals [26,39]. For the above reasons, the fraction of HpCDD (HpCDF) and HxCDD (HxCDF) decreased and the relative amount of low-chlorinated PCDD/Fs increased, and this is why increasing CaO or $CaCO_3$ makes the inhibition efficiency of high chlorinated homologues higher than that of low chlorinated homologues.

In this study, perchlorinated homologues exhibited various destruction percentages. The distribution proportion of OCDD increased after increasing CaO or $CaCO_3$, while that of OCDF barely changed. It has been revealed that TCDD and OCDD are predominantly produced through precursors. The process of TCDD and OCDD formation are mainly condensation and dechlorination reactions, accompanying the production of HCl [30]. The consumption of HCl via Equations (6) and (8) will prominently facilitate the condensation and dechlorination, producing more TCDD and OCDD [30]. Some researchers have used the acid–base interaction in Figure 7 to conjecture the boost impact on PCDD that would be generated from pentachlorophenol (PCP) at 850 °C [30], since the anion could

serve as middle products in PCP condensation. Obviously, the latter hypothesis has been proven in present experiments.

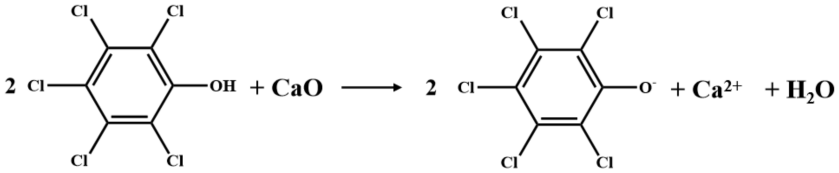

Figure 7. Schematic diagram of acid–base interaction. Reprinted with permission from Elsevier, 2022 [30].

In summary, there is a different impact on PCDDs and PCDFs after increasing CaO or $CaCO_3$ in the sinter raw mix. The de novo synthesis from original materials (C, O, Cl) is inhibited by diminishing the concentrations of the chlorine source and weakening the catalytic activities of metal salt ($CuCl_2$, etc.) to suppress the chlorination of carbon. Dechlorination such as hydrodechlorination also contributes to the inhibition, but is not a major pathway. TCDD and OCDD are predominantly produced through precursors, resulting in the increased distribution proportion of TCDD and OCDD, as shown in Figure 8. Therefore, poisoning catalytic metals or diminishing the chlorine concentration is the dominant route to inhibiting the formation of dioxins during co-sintering with MSWI fly ash by adjusting the sinter raw mix. More experiments need to be further conducted to verify the effectiveness in a real commercial sinter plant and the detailed mechanisms of adjusting the sinter raw mix to inhibit PCDD/F formation in the flue gas.

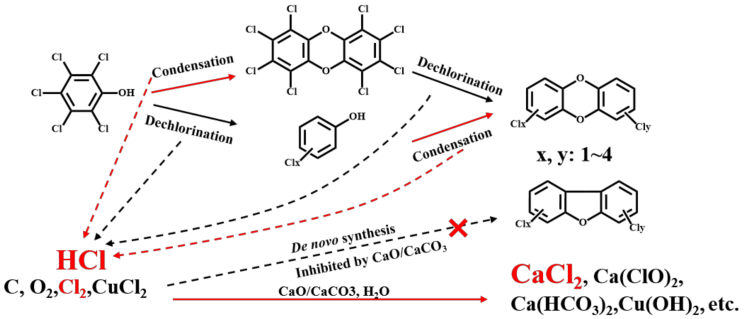

Figure 8. Condensation, dichlorination, and inhibition of PCDD/Fs during co-sintering with MSWI fly ash.

4. Conclusions

In the present research, adjusting the sinter raw mix was proposed as a inhibitory method to inhibit the formation of PCDD/Fs during iron ore co-sintering with MSWI fly ash, based on the mechanism of alkali-base inhibitors, namely, the poisoning of catalytic metals or diminishing the chlorine concentration. The main conclusions are as follows:

(1) After the proportion of calcined lime or limestone in the sinter raw mix slightly increased (1 wt.%, 2 wt.%) within the normal range, the international total toxicity equivalent concentration of dioxins was reduced by 68.22–92.70%. All 2,3,7,8-substituted PCDD/F congeners were inhibited, but the inhibition efficiency of PCDF was higher than that of PCDDs. Furthermore, 5 wt.% calcined lime with 3 wt.% limestone was the best condition for inhibiting the formation of PCDD/Fs.

(2) With the increase in calcined lime or limestone, the distribution proportion of low-chlorinated PCDDs and PCDFs increased, while high-chlorinated PCDDs and PCDFs decreased, except for OCDD. The reason is that the consumption of HCl dramatically promotes the condensation and dechlorination and produces more TCDD and OCDD through precursors, which accompany the production of HCl.

(3) The de novo synthesis from original materials (C, O, Cl) was inhibited by diminishing the concentrations of the chlorine source and weakening the catalytic activities of

metal salt ($CuCl_2$, etc.) to suppress the chlorination of carbon, so condensation and dechlorination are facilitated, causing the increased distribution proportion of TCDD and OCDD.

The results show that co-sintering with MSWI fly ash is feasible. Although dioxins in flue gas increased as fly ash was added, adjusting the sinter raw mixture could make it meet the emissions standards. Further research will explore more efficient additives to inhibit the emission of dioxins in flue gas and the industrialization of co-sintering.

Author Contributions: Conceptualization, S.L. and M.T.; Methodology, Y.P.; Validation, H.H., X.G. and L.J.; Formal analysis, Y.P.; Investigation, H.H.; Resources, Y.P., M.T. and S.L.; Data curation, X.G.; Writing—original draft preparation, H.H.; Writing—review and editing, H.H., X.G. and L.J.; Visualization, H.H.; Supervision, Y.P. and M.T.; Project administration, S.L.; Funding acquisition, M.T. All authors have read and agreed to the published version of the manuscript.

Funding: This work was supported by the Science and Technology Project of Zhejiang Province China (No. 2022C03056) and the China Postdoctoral Science Foundation (No. 2020M681851).

Acknowledgments: The authors are grateful to the School of Minerals Processing and Bioengineering, Central South University, which offered the sinter pot, and Chengetai Portia Makwarimba, who provided the language help.

Conflicts of Interest: The authors declare no conflict of interest. The funders had no role in the design of the study; in the collection, analyses, or interpretation of data; in the writing of the manuscript, or in the decision to publish the results.

Abbreviations

PCDDs	Polychlorinated dibenzo-p-dioxins
PCDFs	polychlorinated dibenzofurans
PCDD/Fs	Polychlorinated dibenzo-p-dioxins and polychlorinated dibenzofurans
TCDD	Tetrachlorianted dibenzo-p-dioxins
PeCDD	Pentachlorinated dibenzo-p-dioxins
HxCDD	Hexachlorinated dibenzo-p-dioxins
HpCDD	Heptachlorinated dibenzo-p-dioxins
OCDD	Octachlorianted dibenzo-p-dioxins
TCDF	Tetrachlorianted dibenzofurans
PeCDF	Pentachlorinated dibenzofurans
HxCDF	Hexachlorianted dibenzofurans
HpCDF	Heptachlorinated dibenzofurans
OCDF	Octachlorianted dibenzofurans
MSWI	Municipal solid waste incineration
I-TEQ	Toxic equivalence quantity
FA	Fly ash
XRF	X-ray fluorescence
FG	Flue gas
HRGC	High resolution gas chromatograph
HRMS	High resolution mass spectrum
EPA	Environmental protection agency

References

1. Nelles, M.; Dorn, T.; Wu, K.; Cai, J. Status and Perspectives Of Waste Incineration In China. *Engineering* **2011**, *30*, 53049218.
2. Quina, M.J.; Bordado, J.C.; Quinta-Ferreira, R.M. Treatment and use of air pollution control residues from MSW incineration: An overview. *Waste Manag.* **2008**, *28*, 2097–2121. [CrossRef] [PubMed]
3. Assi, A.; Bilo, F.; Zanoletti, A.; Ponti, J.; Valsesia, A.; La Spina, R.; Zacco, A.; Bontempi, E. Zero-waste approach in municipal solid waste incineration: Reuse of bottom ash to stabilize fly ash. *J. Clean. Production.* **2020**, *245*, 118779. [CrossRef]
4. Quina, M.J.; Bontempi, E.; Bogush, A.; Schlumberger, S.; Weibel, G.; Braga, R.; Funari, V.; Hyks, J.; Rasmussen, E.; Lederer, J. Technologies for the management of MSW incineration ashes from gas cleaning: New perspectives on recovery of secondary raw materials and circular economy. *Sci. Total. Environ.* **2018**, *635*, 526–542. [CrossRef] [PubMed]

5. Quina, M.J.; Bordado, J.C.M.; Quinta-Ferreira, R.M. Chemical stabilization of air pollution control residues from municipal solid waste incineration. *J. Hazard. Mater.* **2010**, *179*, 382–392. [CrossRef]
6. Zhao, K.; Hu, Y.; Tian, Y.; Chen, D.; Feng, Y. Chlorine removal from MSWI fly ash by thermal treatment: Effects of iron/aluminum additives. *J. Environ. Sci.* **2020**, *88*, 112–121. [CrossRef]
7. Peng, Z.; Weber, R.; Ren, Y.; Wang, J.; Sun, Y.; Wang, L. Characterization of PCDD/Fs and heavy metal distribution from municipal solid waste incinerator fly ash sintering process. *Waste Manag.* **2020**, *103*, 260–267. [CrossRef]
8. Gao, J.; Dong, C.; Zhao, Y.; Hu, X.; Qin, W.; Wang, X.; Zhang, J.; Xue, J.; Zhang, X. Vitrification of municipal solid waste incineration fly ash with B_2O_3 as a fluxing agent. *Waste Manag.* **2020**, *10*, 932–938. [CrossRef] [PubMed]
9. Deng, D.; Qiao, J.; Liu, M.; Kołodyńska, D.; Zhang, M.; Dionysiou, D.D.; Ju, Y.; Ma, J.; Chang, M.B. Detoxification of municipal solid waste incinerator (MSWI) fly ash by single-mode microwave (MW) irradiation: Addition of urea on the degradation of Dioxin and mechanism. *J. Hazard. Mater.* **2019**, *369*, 279–289. [CrossRef] [PubMed]
10. Lindberg, D.; Molin, C.; Hupa, M. Thermal treatment of solid residues from WtE units: A review. *Waste Manag.* **2015**, *37*, 82–94. [CrossRef]
11. Chen, L.; Wang, L.; Cho, D.-W.; Tsang, D.C.W.; Tong, L.; Zhou, Y.; Yang, J.; Hu, Q.; Poon, C.S. Sustainable stabilization/solidification of municipal solid waste incinerator fly ash by incorporation of green materials. *J. Clean. Prod.* **2019**, *222*, 335–343. [CrossRef]
12. Chen, Y.-C.; Kuo, Y.-C.; Chen, M.-R.; Wang, Y.-F.; Chen, C.-H.; Lin, M.-Y.; Yoon, C.; Tsai, P.-J. Reducing polychlorinated dibenzo-p-dioxins and dibenzofurans (PCDD/F) emissions from a real-scale iron ore sinter plant by adjusting its sinter raw mix. *J. Clean. Prod.* **2015**, *112*, 1184–1189. [CrossRef]
13. Long, H.-M.; Zhang, X.-Y.; Li, J.-X.; Wang, P.; Meng, Q.-M.; Gao, Z.-F.; Chun, T.; Wu, X.-J. Study on Emission Characteristics of SO_2 and Feasibility of Desulfurization in Iron Ore Sintering Process. *Chin. J. Process. Eng.* **2015**, *15*, 230–235.
14. Min, Y.; Liu, C.; Shi, P.; Qin, C.; Feng, Y.; Liu, B. Effects of the addition of municipal solid waste incineration fly ash on the behavior of polychlorinated dibenzo-p-dioxins and furans in the iron ore sintering process. *Waste Manag.* **2018**, *77*, 287–293. [CrossRef]
15. Hu, Y.; Zhang, P.; Chen, D.; Zhou, B.; Li, J.; Li, X. Hydrothermal treatment of municipal solid waste incineration fly ash for dioxin decomposition. *J. Hazard. Mater.* **2012**, *207*, 79–85. [CrossRef]
16. Chen, Z.; Zhang, S.; Lin, X.; Li, X. Decomposition and Reformation Pathways of PCDD/Fs during Thermal Treatment of Municipal Solid Waste Incineration Fly Ash. *J. Hazard. Mater.* **2020**, *394*, 122526. [CrossRef]
17. Li, S.; Liu, G.; Zheng, M.; Li, J.; Wang, M.; Li, C.; Chen, Y. Unintentional production of persistent chlorinated and brominated organic pollutants during iron ore sintering processes. *J. Hazard. Mater.* **2017**, *331*, 63–70. [CrossRef] [PubMed]
18. Tan, Y.; Dai, F.; Li, X.; Yu, Y.; He, X.; Chen, D. Inhibitory effect of carbohydrazide on PCDD/Fs formation in iron ore sintering process. *Environ. Pollut. Control* **2012**, *325*, 83–94.
19. Mckay, G. Dioxin characterisation, formation and minimisation during municipal solid waste (MSW) incineration: Review. *Chem. Eng. J.* **2002**, *86*, 343–368. [CrossRef]
20. Fujimori, T.; Toda, A.; Mukai, K.; Takaoka, M. Incineration of carbon nanomaterials with sodium chloride as a potential source of PCDD/Fs and PCBs. *J. Hazard. Mater.* **2020**, *382*, 121030. [CrossRef]
21. Fujimori, T.; Takaoka, M.; Takeda, N. Influence of Cu, Fe, Pb, and Zn Chlorides and Oxides on Formation of Chlorinated Aromatic Compounds in MSWI Fly Ash. *Environ. Sci. Technol.* **2009**, *43*, 8053–8059. [CrossRef] [PubMed]
22. Zhang, M.; Yang, J.; Buekens, A.; Olie, K.; Li, X. PCDD/F catalysis by metal chlorides and oxides. *Chemosphere Environ. Toxicol. Risk Assess.* **2016**, *159*, 536–544. [CrossRef]
23. Wong, G.; Fan, X.; Gan, M.; Ji, Z.; Ye, H.; Zhou, Z.; Wang, Z. Resource utilization of municipal solid waste incineration fly ash in iron ore sintering process: A novel thermal treatment. *J. Clean. Prod.* **2020**, *263*, 121400. [CrossRef]
24. Qian, L.; Chun, T.; Long, H.; Li, J.; Di, Z.; Meng, Q.; Wang, P. Emission reduction research and development of PCDD/Fs in the iron ore sintering. *Process. Saf. Environ. Prot.* **2018**, *117*, 82–91. [CrossRef]
25. Ooi, T.C.; Lu, L. Formation and mitigation of PCDD/Fs in iron ore sintering. *Chemosphere* **2011**, *85*, 291–299. [CrossRef] [PubMed]
26. Wang, Y.; Qian, L.; Yu, Z.; Chun, T.; Long, H.; Wu, X.; Li, J. Inhibition Behavior of PCDD/Fs Congeners by Addition of N-containing Compound in the Iron Ore Sintering. *Aerosol Air Qual. Res.* **2020**, *20*, 2568–2579. [CrossRef]
27. Kasama, S.; Yamamura, Y.; Watanabe, K. Investigation on the dioxin emission from a commercial sintering plant. *ISIJ Int.* **2006**, *46*, 1014–1019. [CrossRef]
28. Ooi, T.C.; Aries, E.; Ewan, B.C.R.; Thompson, D.; Anderson, D.R.; Fisher, R.; Fray, T.; Tognarelli, D. The study of sunflower seed husks as a fuel in the iron ore sintering process. *Miner. Eng.* **2008**, *21*, 167–177. [CrossRef]
29. Liu, W.; Zheng, M.; Zhang, B.; Qian, Y.; Ma, X.; Liu, W. Inhibition of PCDD/Fs formation from dioxin precursors by calcium oxide. *Chemosphere* **2005**, *60*, 785–790. [CrossRef]
30. Lu, S.Y.; Chen, T.; Yan, J.H.; Li, X.D.; Ni, Y.L.M.J.; Cen, K.F. Effects of calcium-based sorbents on PCDD/F formation from pentachlorophenol combustion process. *J. Hazard. Mater.* **2007**, *147*, 663–671. [CrossRef]
31. Chen, Z.; Chang, W.; Jiang, X.; Lu, S.; Buekens, A.; Yan, J. Behavior of Circulating Fluidised Bed MSWI Air Pollution Control Residue in Washing Process. *Energies* **2016**, *9*, 743. [CrossRef]
32. He, H.; Lu, S.; Peng, Y.; Tang, M.; Zhan, M.; Lu, S.; Xu, L.; Zhong, W.; Xu, L. Emission characteristics of dioxins during iron ore Co-sintering with municipal solid waste incinerator fly ash in a sintering pot. *Chemosphere* **2022**, *287*, 131884. [CrossRef] [PubMed]

33. Gan, M.; Ji, Z.; Fan, X.; Chen, X.; Zhou, Y.; Wang, G.; Tian, Y.; Jiang, T. Clean recycle and utilization of hazardous iron-bearing waste in iron ore sintering process. *J. Hazard. Mater.* **2018**, *353*, 381–392. [CrossRef] [PubMed]
34. Medici, F.; Piga, L.; Rinaldi, G. Behaviour of polyaminophenolic additives in the granulation of lime and fly-ash. *Waste Manag.* **2000**, *20*, 491–498. [CrossRef]
35. Gan, M.; Wong, G.; Fan, X.; Ji, Z.; Ye, H.; Zhou, Z.; Wang, Z. Enhancing the degradation of dioxins during the process of iron ore sintering co-disposing municipal solid waste incineration fly ash. *J. Clean. Prod.* **2021**, *291*, 125286. [CrossRef]
36. Chen, Z.; Mao, Q.; Lu, S. Dioxins degradation and reformation during mechanochemical treatment. *Chemosphere* **2017**, *180*, 130–140. [CrossRef]
37. Wu, H.-L.; Lu, S.-Y.; Li, X.-D.; Jiang, X.-G.; Yan, J.-H.; Zhou, M.-S.; Wang, H. Inhibition of PCDD/F by adding sulphur compounds to the feed of a hazardous waste incinerator. *Chemosphere* **2012**, *86*, 361–367. [CrossRef]
38. Huang, H.; Buekens, A. On the mechanisms of dioxin formation in combustion processes. *Chemosphere* **1995**, *31*, 4099–4117. [CrossRef]
39. Ma, H.; Du, N.; Lin, X.; Liu, C.; Zhang, J.; Miao, Z. Inhibition of element sulfur and calcium oxide on the formation of PCDD/Fs during co-combustion experiment of municipal solid waste. *Sci. Total. Environ.* **2018**, *633*, 1263–1271. [CrossRef]
40. Lin, Y.-S.; Chen, K.-S.; Lin, Y.-C.; Hung, C.-H.; Chang-Chien, G.-P. Polychlorinated dibenzo-p-dioxins/dibenzofurans distributions in ash from different units in a municipal solid waste incinerator. *J. Hazard. Mater.* **2008**, *154*, 954–962. [CrossRef]
41. Gullett, B.K.; Bruce, K.R.; Beach, L.O.; Drago, A.M. Mechanistic steps in the production of PCDD and PCDF during waste combustion. *Chemosphere* **1992**, *25*, 1387–1392. [CrossRef]
42. Olie, K.; Addink, R.; Schoonenboom, M. Metals as Catalysts during the Formation and Decomposition of Chlorinated Dioxins and Furans in Incineration Processes. *Air Repair* **1998**, *48*, 101–105. [CrossRef]
43. Tabata, M.; Ghaffar, A.; Shono, A.; Notomi, K. Hydrodechlorination/detoxification of PCDDs, PCDFs, and co-PCBs in fly ash by using calcium polysulfide. *Waste Manag.* **2013**, *33*, 356–362. [CrossRef] [PubMed]
44. Altarawneh, M.; Dlugogorski, B.Z.; Kennedy, E.M.; Mackie, J.C. Mechanisms for formation, chlorination, dechlorination and destruction of polychlorinated dibenzo-p-dioxins and dibenzofurans (PCDD/Fs). *Prog. Energy Combust. Sci.* **2009**, *35*, 245–274. [CrossRef]
45. Yang, Z.J.; Xia, C.H.; Zhang, Q.; Chen, J.P.; Wu, W.Z.; Liang, X.M.; Kettrup, A. Treatment of PCDD/Fs and PCBs in fly ash extracts under mild conditions. *Fresenius Environ. Bull.* **2006**, *15*, 86–94.
46. Zhang, Q.; Liang, X.M.; Xu, J.; Chen, J.P.; Lu, P.Z. Chemical Dechlorination of PCB in Transformer Oil by Use of Nano-NaH and Its Assessment. *Fine Chem.* **2004**, *7*, 540–543.
47. Lu, G.-N.; Dang, Z.; Fennell, D.E.; Huang, W.; Li, Z.; Liu, C.-Q. Rules of thumb for assessing reductive dechlorination pathways of PCDDs in specific systems. *J. Hazard. Mater.* **2010**, *177*, 1145–1149. [CrossRef]